Research Article | Vol. 26, No. 14 | 9 Jul 2018 | OPTICS EXPRESS 18699
Optics EXPRESS

Laser frequency instability of 2×10^{-16} by stabilizing to 30-cm-long Fabry-Pérot cavities at 578 nm

LI JIN,[1] YANYI JIANG,[1,2,3] YUAN YAO,[1,4] HONGFU YU,[1] ZHIYI BI,[1] AND LONGSHENG MA[1,2]

[1]*State Key Laboratory of Precision Spectroscopy, East China Normal University, Shanghai 200062, China*
[2]*Collaborative Innovation Center of Extreme Optics, Shanxi University, Taiyuan, Shanxi 030006, China*
[3]*yyjiang@phy.ecnu.edu.cn*
[4]*yyao@lps.ecnu.edu.cn*

Abstract: Laser light at 578 nm is frequency-stabilized to two independent 30-cm-long Fabry-Pérot cavities. To achieve a thermal-noise-limited cavity length stability, the geometry and support configuration of the Fabry-Pérot cavities are optimized. The fractional frequency instability of each cavity-stabilized laser system is 2×10^{-16} at 1 s averaging time, approaching to the thermal-noise-induced length instability of the reference cavity. The most probable linewidth of each laser system is about 0.2 Hz, and the laser frequency noise at Fourier frequency of 1 Hz is 0.1 Hz/√Hz.

OCIS codes: (140.3425) Laser stabilization; (120.2230) Fabry-Perot; (300.3700) Linewidth; (300.6320) Spectroscopy, high-resolution; (120.3940) Metrology.

References and links

1. A. D. Ludlow, M. M. Boyd, J. Ye, E. Peik, and P. O. Schmidt, "Optical atomic clocks," Rev. Mod. Phys. **87**(2), 637–701 (2015).
2. T. L. Nicholson, S. L. Campbell, R. B. Hutson, G. E. Marti, B. J. Bloom, R. L. McNally, W. Zhang, M. D. Barrett, M. S. Safronova, G. F. Strouse, W. L. Tew, and J. Ye, "Systematic evaluation of an atomic clock at 2×10^{-18} total uncertainty," Nat. Commun. **6**(1), 6896 (2015).
3. M. Schioppo, R. C. Brown, W. F. McGrew, N. Hinkley, R. J. Fasano, K. Beloy, T. H. Yoon, G. Milani, D. Nicolodi, J. A. Sherman, N. B. Phillips, C. W. Oates, and A. D. Ludlow, "Ultrastable optical clock with two cold-atom ensembles," Nat. Photonics **11**(1), 48–52 (2017).
4. R. X. Adhikari, "Gravitational radiation detection with laser interferometry," Rev. Mod. Phys. **86**(1), 121–151 (2014).
5. T. M. Fortier, M. S. Kirchner, F. Quinlan, J. Taylor, J. C. Bergquist, T. Rosenband, N. Lemke, A. Ludlow, Y. Jiang, C. W. Oates, and S. A. Diddams, "Generation of ultrastable microwaves via optical frequency division," Nat. Photonics **5**(7), 425–429 (2011).
6. Y. Yao, Y. Jiang, L. Wu, H. Yu, Z. Bi, and L. Ma, "A low noise optical frequency synthesizer at 700–990nm," Appl. Phys. Lett. **109**(13), 131102 (2016).
7. S. Herrmann, A. Senger, K. Möhle, M. Nagel, E. V. Kovalchuk, and A. Peters, "Rotating optical cavity experiment testing Lorentz invariance at the 10^{-17} level," Phys. Rev. D Part. Fields Gravit. Cosmol. **80**(10), 105011 (2009).
8. Y. Y. Jiang, A. D. Ludlow, N. D. Lemke, R. W. Fox, J. A. Sherman, L.-S. Ma, and C. W. Oates, "Making optical atomic clocks more stable with 10^{-16}-level laser stabilization," Nat. Photonics **5**(3), 158–161 (2011).
9. S. Doeleman, T. Mai, A. E. E. Rogers, J. G. Hartnett, M. E. Tobar, and N. Nand, "Adapting a cryogenic sapphire oscillator for very long baseline interferometry," Publ. Astron. Soc. Pac. **123**(903), 582–595 (2011).
10. J. M. Hogan and M. A. Kasevich, "Atom-interferometric gravitational-wave detection using heterodyne laser links," Phys. Rev. A **94**(3), 033632 (2016).
11. S. Grop, P. Y. Bourgeois, N. Bazin, Y. Kersalé, E. Rubiola, C. Langham, M. Oxborrow, D. Clapton, S. Walker, J. De Vicente, and V. Giordano, "ELISA: a cryocooled 10 GHz oscillator with 10^{-15} frequency stability," Rev. Sci. Instrum. **81**(2), 025102 (2010).
12. R. W. P. Drever, J. L. Hall, F. V. Kowalski, J. Hough, G. M. Ford, A. J. Munley, and H. Ward, "Laser phase and frequency stabilization using an optical resonator," Appl. Phys. B **31**(2), 97–105 (1983).
13. B. C. Young, F. C. Cruz, W. M. Itano, and J. C. Bergquist, "Visible lasers with subhertz linewidths," Phys. Rev. Lett. **82**(19), 3799–3802 (1999).

#332205 https://doi.org/10.1364/OE.26.018699
Journal © 2018 Received 5 Jun 2018; accepted 11 Jun 2018; published 5 Jul 2018

Optics EXPRESS

14. M. J. Martin, D. Meiser, J. W. Thomsen, J. Ye, and M. J. Holland, "Extreme nonlinear response of ultranarrow optical transitions in cavity QED for laser stabilization," Phys. Rev. A **84**(6), 063813 (2011).
15. P. G. Westergaard, B. T. R. Christensen, D. Tieri, R. Matin, J. Cooper, M. Holland, J. Ye, and J. W. Thomsen, "Observation of motion-dependent nonlinear dispersion with narrow-linewidth atoms in an optical cavity," Phys. Rev. Lett. **114**(9), 093002 (2015).
16. J. B. Chen, "Active optical clock," Chin. Sci. Bull. **54**(3), 348–352 (2009).
17. M. A. Norcia, M. N. Winchester, J. R. K. Cline, and J. K. Thompson, "Superradiance on the millihertz linewidth strontium clock transition," Sci. Adv. **2**(10), e1601231 (2016).
18. J. M. Weiner, K. C. Cox, J. G. Bohnet, and J. K. Thompson, "Phase synchronization inside a superradiant laser," Phys. Rev. A **95**(3), 033808 (2017).
19. K. Numata, A. Kemery, and J. Camp, "Thermal-noise limit in the frequency stabilization of lasers with rigid cavities," Phys. Rev. Lett. **93**(25), 250602 (2004).
20. S. Häfner, S. Falke, C. Grebing, S. Vogt, T. Legero, M. Merimaa, C. Lisdat, and U. Sterr, "8×10^{-17} fractional laser frequency instability with a long room-temperature cavity," Opt. Lett. **40**(9), 2112–2115 (2015).
21. T. L. Nicholson, M. J. Martin, J. R. Williams, B. J. Bloom, M. Bishof, M. D. Swallows, S. L. Campbell, and J. Ye, "Comparison of two independent Sr optical clocks with 1×10^{-17} stability at 10^3 s," Phys. Rev. Lett. **109**(23), 230801 (2012).
22. G. M. Harry, A. M. Gretarsson, P. R. Saulson, S. E. Kittelberger, S. D. Penn, W. J. Startin, S. Rowan, M. M. Fejer, D. R. M. Crooks, G. Cagnoli, J. Hough, and N. Nakagawa, "Thermal noise in interferometric gravitational wave detectors due to dielectric optical coatings," Class. Quantum Gravity **19**(5), 897–917 (2002).
23. G. D. Cole, W. Zhang, M. J. Martin, J. Ye, and M. Aspelmeyer, "Tenfold reduction of Brownian noise in high-reflectivity optical coatings," Nat. Photonics **7**(8), 644–650 (2013).
24. D. G. Matei, T. Legero, S. Häfner, C. Grebing, R. Weyrich, W. Zhang, L. Sonderhouse, J. M. Robinson, J. Ye, F. Riehle, and U. Sterr, "1.5 μm lasers with sub-10 mHz linewidth," Phys. Rev. Lett. **118**(26), 263202 (2017).
25. W. Zhang, J. M. Robinson, L. Sonderhouse, E. Oelker, C. Benko, J. L. Hall, T. Legero, D. G. Matei, F. Riehle, U. Sterr, and J. Ye, "Ultrastable silicon cavity in a continuously operating closed-cycle cryostat at 4 K," Phys. Rev. Lett. **119**(24), 243601 (2017).
26. A. Noack, C. Bogan, and B. Willke, "Higher-order Laguerre-Gauss modes in (non-) planar four-mirror cavities for future gravitational wave detectors," Opt. Lett. **42**(4), 751–754 (2017).
27. X. Y. Zeng, Y. X. Ye, X. H. Shi, Z. Y. Wang, K. Deng, J. Zhang, and Z. H. Lu, "Thermal-noise-limited higher-order mode locking of a reference cavity," Opt. Lett. **43**(8), 1690–1693 (2018).
28. B. Argence, E. Prevost, T. Lévèque, R. Le Goff, S. Bize, P. Lemonde, and G. Santarelli, "Prototype of an ultra-stable optical cavity for space applications," Opt. Express **20**(23), 25409–25420 (2012).
29. J. Millo, D. V. Magalhães, C. Mandache, Y. Le Coq, E. M. L. English, P. G. Westergaard, J. Lodewyck, S. Bize, P. Lemonde, and G. Santarelli, "Ultrastable lasers based on vibration insensitive cavities," Phys. Rev. A **79**(5), 053829 (2009).
30. Y. Li, Y. G. Lin, Q. Wang, T. Yang, Z. Sun, E. Zang, and Z. J. Fang, "An improved strontium lattice clock with 10^{-16} level laser frequency stabilization," Chin. Opt. Lett. **16**(5), 051402 (2018).
31. Z. Tai, L. Yan, Y. Zhang, X. Zhang, W. Guo, S. Zhang, and H. Jiang, "Transportable 1555-nm ultra-stable laser with sub-0.185-Hz linewidth," Chin. Phys. Lett. **34**(9), 090602 (2017).
32. T. Legero, T. Kessler, and U. Sterr, "Tuning the thermal expansion properties of optical reference cavities with fused silica mirrors," J. Opt. Soc. Am. B **27**(5), 914–919 (2010).
33. J. Ye and J. L. Hall, "Cavity ringdown heterodyne spectroscopy: High sensitivity with microwatt light power," Phys. Rev. A **61**(6), 061802 (2000).
34. L. S. Ma, P. Jungner, J. Ye, and J. L. Hall, "Delivering the same optical frequency at two places: accurate cancellation of phase noise introduced by an optical fiber or other time-varying path," Opt. Lett. **19**(21), 1777–1779 (1994).
35. L. Chen, J. L. Hall, J. Ye, T. Yang, E. Zang, and T. Li, "Vibration-induced elastic deformation of Fabry-Perot cavities," Phys. Rev. A **74**(5), 053801 (2006).
36. M. Notcutt, L. S. Ma, J. Ye, and J. L. Hall, "Simple and compact 1-Hz laser system via an improved mounting configuration of a reference cavity," Opt. Lett. **30**(14), 1815–1817 (2005).
37. Y. Jiang, S. Fang, Z. Bi, X. Xu, and L. Ma, "Nd:YAG lasers at 1064 nm with 1-Hz linewidth," Appl. Phys. B **98**(1), 61–67 (2010).

1. Introduction

Benefitting from high phase coherence, spectrally-narrow ultra-stable lasers are essential to precision spectroscopy, optical atomic clocks [1–3], gravitational wave detection [4], generation of low-phase-noise microwave signals [5], low-noise optical frequency synthesizer [6], and tests of fundamental physics [7]. To fully meet the demands of those applications, the pursuit for lasers with even higher frequency stability and coherence has never stopped. Taking optical atomic clocks as an example, when the frequency instability of ultra-stable lasers as local oscillators is reduced from 10^{-15} to 10^{-16}, the frequency stability of optical

Optics EXPRESS

clocks has been improved from $10^{-15}/\sqrt{\tau}$ to $10^{-16}/\sqrt{\tau}$ (τ is the averaging time) [8], enabling 10^{-18} frequency instability in an averaging time of less than one day. Further improvements on ultra-stable lasers will open up new applications in sub-mm very long baseline interferometry (VLBI), atom interferometry, and deep space navigation [9–11].

To achieve high phase coherence and frequency stability, the phase/frequency noise of lasers is usually eliminated by frequency-stabilizing to a spectrally narrow and stable frequency reference such as a high-finesse Fabry-Pérot (F-P) cavity or a narrow-linewidth atomic transition [12–15]. Alternative ways are explored to generate spectrally-narrow, ultra-stable laser light directly from a superradiant laser [16–18]. So far, the most popular way to achieve narrow-linewidth ultra-stable laser light is to stabilize the laser frequency to the resonance of a high-finesse F-P cavity by using the Pound-Drever-Hall (PDH) technique [12]. The frequency noise and frequency stability of those cavity-stabilized lasers are mainly determined by the optical-length stability of the reference cavities. Thermal Brownian noise, as the fundamental physical effect, limits the achievable length stability of F-P cavities [19]. The cavity-thermal-noise-limited laser frequency instability can be improved by increasing the cavity length [8,20,21], using low mechanical loss materials for mirror substrates and coatings [22,23], reducing the cavity temperature [24,25] or increasing the beam size on the cavity mirrors [3,26,27]. By combining some of those methods, some ultra-stable lasers reach a frequency instability of 10^{-16} and better [8,13,20,25,28–31], and those frequency-stabilized to cryogenic F-P cavities achieve 10^{-17} frequency instability at 1 s averaging time [24].

In this paper, we construct two high-finesse F-P cavities at 578 nm in room temperature. To achieve a thermal-noise-limited cavity length instability at the 10^{-16} level, the cavity length is increased to 30 cm, and two fused silica (FS) mirrors with lower mechanical loss, in comparison to ultralow-expansion (ULE) glass, are optically contacted to the cavity ends. According to Refs [19]. and [23], the cavity-thermal-noise-limited laser frequency instability and laser frequency noise at Fourier frequency of 1 Hz are estimated to be 1.6×10^{-16} and 0.06 Hz/√Hz, respectively. For the frequency noise at Fourier frequency of 1 Hz, the Brownian motion of the mirror coating and the coating thermos-elastic noise are the two biggest contributions, 75% and 14% over all the cavity thermal noise. Laser light at 578 nm is independently frequency-stabilized to the resonance of each reference cavity. To achieve a cavity-thermal-noise-limited performance, we evaluated and reduced the laser frequency noise induced by seismic vibration, light power fluctuation and residual amplitude modulation (RAM) of the light. Measurements show that each laser system has a fractional frequency instability of 2×10^{-16} at 1 s averaging time and a frequency noise of 0.1 Hz/√Hz at Fourier frequency of 1 Hz, approaching to the cavity-thermal-noise-limited performance. Since the laser frequency instability contributed by cavity vibration is about the same level as that contributed by the cavity thermal noise, the measured laser frequency instability varies with surrounding vibration noise, about $(2–3) \times 10^{-16}$ during the daytime.

2. Experimental setup

The schematic diagram of the experimental setup for laser frequency stabilization is shown in Fig. 1. Each cavity spacer, made of ULE glass, is cylindrical. There are two cutouts below its mid-plane for supporting. Each cavity is horizontally supported on four Viton hemispheres with a diameter of 6 mm. The hemispheres sit on a U-shape support made of ULE glass. Two FS mirrors with curvature of $R_1 = \infty$ and $R_2 = 1$ m are optically contacted to the ends of the 30-cm-long cylindrical spacer. An additional ULE ring is optically contacted to the rear surface of each FS mirror to reduce the mirror bending due to the coefficient of thermal expansions (CTE) mismatch between the mirrors and the spacer [32].

The finesses of the F-P cavities are measured to be 154,000 for CAV1 and 96,000 for CAV2 from the cavity-field-ring down signal by heterodyne detecting the cavity reflection [33]. To reduce the sensitivity of the F-P cavities to environmental thermal fluctuation, each

Optics EXPRESS

cavity and its support are enclosed in two layers of gold-plated copper shields inside a vacuum chamber made of aluminum. The vacuum chamber is evacuated down to 10^{-7} torr. Thermal radiation dominates in heat transfer between the vacuum chambers and the F-P cavities. The response time for each F-P cavity to the temperature change of the vacuum chamber is measured to be nearly 150 hours. For the convenience temperature control using heaters, the vacuum chambers outside the cavities are temperature-stabilized at about 26 °C with a fluctuation below 1.5 mK. In order to reduce the vibration-induced cavity length fluctuation, each vacuum chamber and the optics for the PDH technique are placed on an active vibration isolation platform. Outside them, there is a box made of aluminum plates covered with acoustic absorbing material to reduce the disturbance of air flow and surrounding acoustic noise. The two cavity systems are independent: one cavity system is placed on an optical platform while the other is on the floor. They are about 5 meters apart.

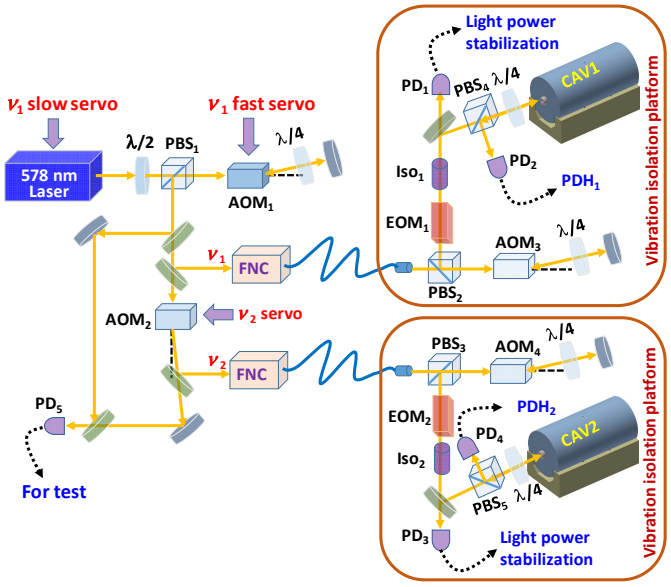

Fig. 1. Schematic diagram of the experimental setup for laser frequency stabilization and laser performance measurement. The PDH_1 (PDH_2) signal is fed back to ν_1 slow servo and ν_1 fast servo (ν_2 servo). λ/2, half-wave plate. PBS, polarization beam splitter. AOM, acousto-optic modulator. FNC, fiber noise cancellation. EOM, electro-optic modulator. Iso, optical isolator. λ/4, quarter-wave plate. PD, photo-detector.

Laser light at 578 nm is separately frequency-stabilized to the resonance of each ultra-stable optical reference cavity. The 578 nm laser light is generated by summing from the light of a 1030 nm fiber laser and a 1319 nm Nd:YAG laser. The 578 nm laser light firstly double-passes an acousto-optic modulator (AOM_1), which is used for fast laser frequency control with a servo bandwidth up to 175 kHz. Then the light is split into four parts. One part with frequency of ν_1 is transferred via a polarization-maintaining (PM) fiber to CAV1 for laser frequency stabilization by controlling the driving frequency of AOM_1 and the voltage of a piezo (PZT) inside the laser with the PDH_1 signal. Additional undesirable random phase noise arising from the PM fiber is suppressed with fiber noise cancellation (FNC) technique [34]. The second part passes through AOM_2. The first-order diffraction light of AOM_2 with frequency of ν_2 is then sent to CAV2 via a second PM fiber. The PDH_2 signal from CAV2 is sent to a servo to tune the driving frequency of AOM_2 for laser frequency stabilization to the resonance of CAV2. The servo bandwidth of AOM_2 is nearly 100 kHz. Parts of the laser light before and after AOM_2 are picked up with beam splitters, and they heterodyne with each other on a photo-detector (PD_5).

Optics EXPRESS

At the output of each PM fiber, the laser light is frequency-shifted by AOM_3 for CAV1 system (or AOM_4 for CAV2 system), whose first-order diffraction efficiency is adjusted by controlling its RF driving power according to the monitor signal from PD_1 (or PD_3) for light power stabilization. Then the diffraction laser light is phase-modulated at the frequency of 22.3 MHz in an electro-optic modulator (EOM, LINOS PM25). The polarization of the light incident onto the EOM is aligned along the principle axis of the EO crystal (ADP) to reduce undesired amplitude modulation. To further reduce the RAM, an optical isolator, Iso_1 (or Iso_2), is placed after the EOM to prevent the light reflected back into the EOM. The cavity reflection contrast is about 50% for both cavities. The light reflected from the reference cavity is focused into PD_2 (or PD_4). Then the RF signal from PD_2 (or PD_4) is demodulated to generate a PDH-based frequency discrimination signal for either laser frequency stabilization or laser frequency noise measurement.

3. Reduction of laser frequency noise

The Residual amplitude modulation in EOM has been identified as a significant source of frequency noise in cavity-stabilized laser systems based on the technique of phase modulation. We separately measured the power spectral density (PSD) of the PDH-based frequency discrimination signals (PDH_1 and PDH_2 as shown in Fig. 1) on a fast Fourier transform (FFT) spectrum analyzer when the laser frequency is far off resonance of the reference cavities. The PSD of the PDH signal in unit of V/√Hz measured on the FFT spectrum analyzer is converted to laser frequency noise with the slope of the PDH signal. The frequency noise at Fourier frequency of 1 Hz is evaluated to be 0.013 Hz/√Hz and 0.022 Hz/√Hz for CAV1 and CAV2 systems, respectively, far less than the laser frequency noise contributed by the cavity thermal noise. This measurement includes the contribution from the RAM and the electrical noise. To measure the long term fluctuation of RAM, the PDH-based frequency discrimination signals are monitored on a high-precision multimeter. It is then converted to laser frequency fluctuation with the slope of the PDH signal. It shows that RAM-induced laser frequency instability is less than 4×10^{-17} at an averaging time of 1 s to 1000 s. Benefitting from the insensitivity of ADP crystal birefringence to temperature fluctuation and the employment of the high extinction ratio polarizer before the EOM and an isolator after the EOM, it is unnecessary to stabilize the temperature of the EOMs or actively compensate the temperature-induced crystal birefringence to reduce the RAM at this level.

The sensitivity of the cavity resonant frequency shift to the power fluctuation of the cavity incident light is measured to be 10 Hz/μW. The power of the light incident into the reference cavity is stabilized to 30 μW with a fractional instability of 4×10^{-5} (1 s) and 5×10^{-5} (100 s). Therefore, light-power-instability-induced laser frequency instability is estimated to be less than 3×10^{-17} at an averaging time of 1-100 s.

Environmental vibration has a significant effect on the cavity length via its supports. It is one of the primary challenges to achieve laser frequency instability below 10^{-15} [13,25,29,35,36]. Moreover, since our laboratory is on top of basements, the amplitude of vibration is larger than those directly constructed on the ground. To evaluate the contribution from vibration, the length sensitivity of two optical cavities to vibration (or cavity vibration sensitivity) is separately measured. The schematic diagram for measuring the cavity vibration sensitivity is shown in Fig. 2(a). Each time we purposely applied shakes with PSD on the order of 10^{-3} g/√Hz along one direction on the active vibration isolation platform of the test cavity. When the light is resonant on the test cavity, the PDH-based frequency discrimination signal from the test cavity is measured on the FFT spectrum analyzer. The PSD of the PDH signal at the shaking frequency is then scaled to laser frequency noise f_i with the slope of the PDH signal. Meanwhile, an accelerometer measures the shaking-induced acceleration of a_i at the shaking frequency. Then the sensitivity of the test cavity to vibration along a certain direction is calculated as $S_i = f_i / (v \times a_i)$, here the subscript $i = x$, y or z denotes the shaking direction and v is the light frequency.

Optics EXPRESS

When designing the geometry of the reference cavities, we did numerical simulations to obtain the fractional length change of an optical cavity under an acceleration. The laser light on resonance of the reference cavity may offset from the mirror center due to the misalignment between the mirror centers and the optical axis of the cavity spacer. Therefore, we adjusted the distances of the support points to the cavity mid-plane in the z direction (h), to the cutouts in the y direction (l) and to the cavity end in the x direction (d) to find an optimal design for a minimized vertical vibration sensitivity as well as a low sensitivity to the offset of light spots from the mirror centers. Figure 2(b) shows the simulated vertical vibration sensitivity as well as the measurement results (shown with filled triangles and dots) when h = 20.9 mm. In simulation, for different l as shown with open squares and circles, it has different optimal d for a minimized vibration sensitivity. The figure shows vertical vibration sensitivity of the light spot at the mirror center (open squares and circles) and those ± 0.2 mm offset from the mirror centers (dot lines). From simulation, when h = 20.9 mm, l = 16 mm and d = 55 mm or l = 8 mm and d = 63 mm, the cavity length for light spots has the lowest vibration sensitivity of 5×10^{-11} /g.

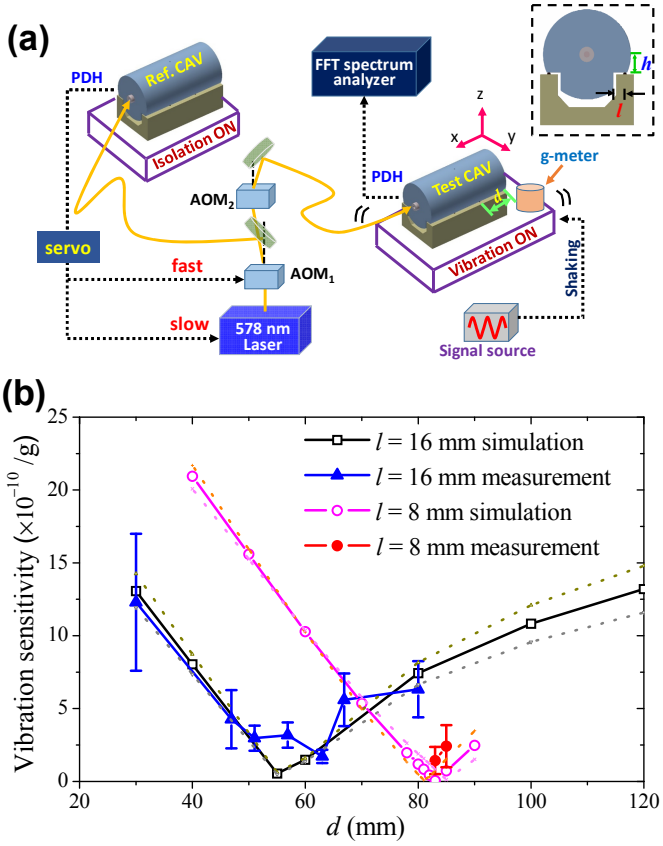

Fig. 2. Vibration sensitivity measurement. (a) Schematic diagram. The laser light is frequency-stabilized to the resonance of the reference cavity. The test cavity is placed on a platform shaking at the testing frequency along one direction. An accelerometer (g-meter) measures the shaking-induced vibration noise on the platform. (b) The vertical vibration sensitivity of the reference cavity at different d and l when h = 20.9 mm. The dot lines are the simulation results of the light spots offset from the center of cavity mirrors by + 0.2 mm and –0.2 mm, while the open squares and circles are the simulation results of the light spots in the center of cavity mirrors. The simulation results are taken the absolute value.

In experiments, the cavity vibration sensitivities along three directions are measured after the test cavity is evacuated and temperature-stabilized. Vertical vibration sensitivity of 2.5 ×

Optics EXPRESS

10^{-10} /g is achieved when the four hemispheres sit at l = 8 mm, d = 63 mm. In simulation, the cavity should be insensitive to horizontal vibration along the x or y direction due to the symmetric geometry. However, the initial measurements show the cavity vibration sensitivity in the horizontal directions was on the order of 10^{-9} /g. To reduce the cavity vibration sensitivity in horizontal directions, we re-supported the cavity in a symmetrical way by using four hemispheres with almost the same height and symmetrically locating the four hemispheres. Meanwhile, we mounted the U-shape supporter rigidly to reduce the vibration-induced unbalanced-deformation of the top surface of the U-shape supporter. With these measures, the cavity sensitivity to horizontal vibration is reduced to less than 5×10^{-10}/g. Table 1 lists the measured vibration sensitivities S_i at the optimized support positions at the shaking frequency of 2 Hz (1 Hz) for CAV1 (CAV2). The measurement uncertainty is from the standard deviation of several measurements. An optimized vibration sensitivity of CAV2 (h = 30 mm) is also achieved when l = 14 mm and d = 100 mm.

Table 1. Vibration sensitivity of optical reference cavities

	Vibration sensitivity S_i ($\times 10^{-10}$ /g)	
	CAV1	CAV2
Vertical (z)	1.1 (0.2)	1.8 (0.3)
Optical axis (x)	2.1 (0.1)	4.4 (0.5)
⊥ optical axis (y)	2.3 (0.1)	0.8 (0.1)

4. Performance evaluation

The laser frequency noise is measured by stabilizing the laser frequency ν_1 to the resonance of CAV1 and measuring the PDH_2 signal from CAV2 on the FFT spectrum analyzer when the laser light with frequency of ν_2 is on resonance of CAV2. The measured laser frequency noise is contributed from the two cavities systems. As shown in Fig. 3(a), for Fourier frequencies below 6 Hz, the laser frequency noise (black solid line) approaches to the combined thermal noise limit from two cavities (green solid line). The vibration-induced laser frequency noise from each reference cavity is also plotted in the figure with dash lines. As we can see in the figure, below Fourier frequency of 6 Hz, the laser frequency noise arisen from cavity thermal noise and that from vibration are about the same. Above 6 Hz, the contribution from cavity vibration dominates the frequency noise of two laser systems.

When the 578 nm laser light with frequency of ν_1 (ν_2) is stabilized to CAV1 (CAV2), the frequency of the beating signal on PD_5 is measured on frequency counters (Agilent 53132 and K + K counter). Meanwhile, we also measured the driving frequency of AOM_2, whose stability is found to be the same as that of the signal from PD_5. After subtracting a linear laser frequency drift rate of 0.02 Hz/s, the fractional frequency instability of the beat note is calculated to be 2.5×10^{-16} at 1 s averaging time, as shown in Fig. 3(b), approaching to the combined cavity-thermal-noise-limited laser frequency instability of 2.3×10^{-16}. Assuming the two laser systems are similar, the frequency instability of each laser system is 1.8×10^{-16} at 1 s averaging time. However, the laser frequency instability at longer times beyond 10 s shows fast degradation mainly due to thermal-induced cavity length fluctuation. Another possibility for the fast degradation of the stability beyond 10 s may come from an imperfect optical contacting between one of the cavity mirrors and its ULE ring, where a bubble is visibly observed. Since the laser frequency instability contributed by cavity vibration is about the same level as the cavity thermal noise, the measured laser frequency instability varies with surrounding vibration noise. Figure 3(c) shows the frequency instability of the beat note at 1 s averaging time over the time of a day. This measurement is performed on several days, and the error bars shown in the figure are the standard deviation of several measurements. At midnight when there is less vibration noise, the laser frequency instability is close to the cavity thermal noise limit. During the daytime, the frequency instability of the beat note is (3–4) $\times 10^{-16}$ at 1 s averaging time, corresponding to (2–3) $\times 10^{-16}$ for each laser.

Optics EXPRESS

The linewidth of the beat note was measured on the FFT spectrum analyzer with a resolution bandwidth of 61 mHz and an acquisition time of 16 s. Each group of spectra was fitted with a Lorentzian function to obtain the linewidth of the beat note. The inset of Fig. 3(d) shows an example of one spectrum with a fitting linewidth of 0.16 Hz. Figure 3(d) shows the linewidth distribution of 894 groups of the spectra taken on four days. The linewidth distribution deviates from normal distribution due to the cutoff at nearly twice the resolution bandwidth of the FFT spectrum analyzer [37]. The probability for observing a beat note linewidth of < 0.5 Hz is 84%. The most probable observed linewidth of the beat note is about 0.3 Hz. We also center-overlapped all the 894 groups of spectra and averaged all the group, as shown in Fig. 3(e). The Lorentzian fitting shows that an averaging linewidth is 0.32 Hz. Based on these measurements, the linewidth of each laser system is estimated to be 0.2 Hz by dividing the linewidth of the beat note by √2.

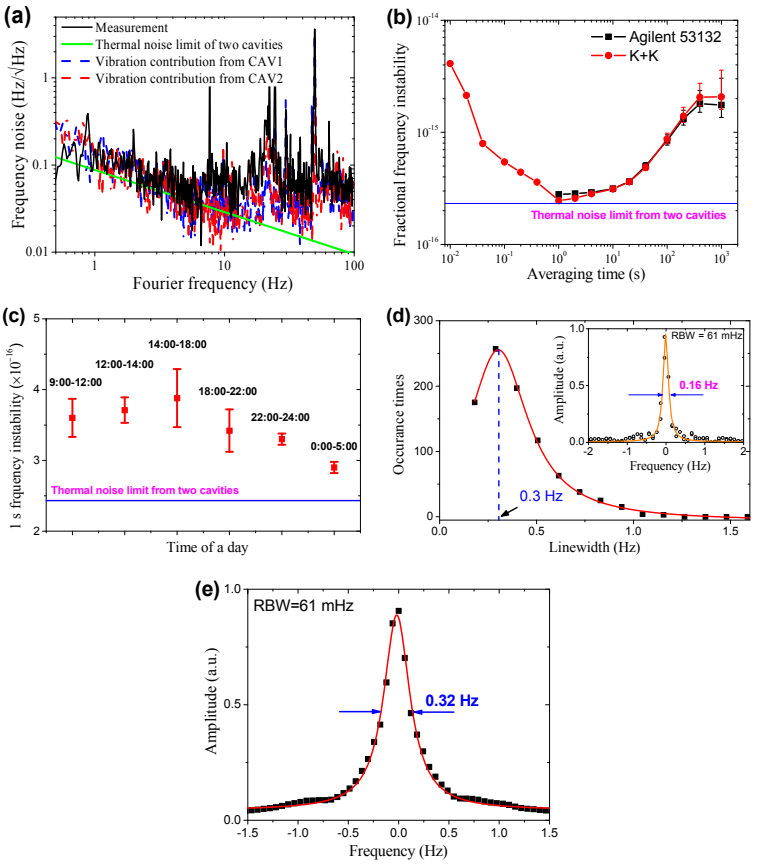

Fig. 3. Performance measurement of the cavity-stabilized laser systems. (a) The frequency noise of two cavity-stabilized laser systems (black solid line). The contribution from the vibration of CAV1 (CAV2) is estimated from the measured vibration sensitivity and vibration acceleration, shown with a blue (red) dash line. The green solid line is the combined thermal-noise-limited laser frequency noise from two cavities. (b) Frequency instability measurement of the beat note between two cavity-stabilized laser systems. The combined thermal-noise-limited laser frequency instability from two cavities is shown with blue solid line. (c) The frequency instability of the beat note between two cavity-stabilized laser systems at 1 s averaging time over the time of a day. The data were taken on different days. The error bars are the standard deviation of several measurements. Each measurement is based on 3600 s data. (d) Linewidth distribution of 896 groups of the beat note spectra (squares) and its Gaussian fitting (red solid curve). The inset shows an example spectrum of the beat note and its Lorentzian fitting. (e) An averaging spectrum of the beat note with center-overlapped (squares) and the Lorentzian fitting (red solid curve).

Optics EXPRESS

5. Conclusion

In conclusion, we report laser light at 578 nm is frequency-stabilized to each of 30-cm long F-P cavities at room temperature. The fractional frequency instability of each laser is 2×10^{-16} at 1 s averaging time, approaching to the cavity-thermal-noise-induced length instability. To push the laser frequency instability to 10^{-17}, the cavity mirrors will be replaced by those with crystalline coating, which has less mechanical loss in comparison to dielectric coating and thus has less thermal noise [23]. For even lower thermal noise of reference cavities, cryogenic F-P cavities will be explored. Moreover, the geometry and supporting configuration of the reference cavities will be redesigned to eliminate the vibration-induced laser frequency noise below the contribution of cavity thermal noise.

Funding

The National Natural Science Foundation of China (91636214, 11654004 and 11334002); National Key R&D Program of China (2017YFA0304403); and the 111 Project (B12024).